Technical Notes

TECHNICAL NOTES are short manuscripts describing new developments or important results of a preliminary nature. These Notes cannot exceed 6 manuscript pages and 3 figures; a page of text may be substituted for a figure and vice versa. After informal review by the editors, they may be published within a few months of the date of receipt. Style requirements are the same as for regular contributions (see inside back cover).

Numerical Studies of the Hypersonic Strong Interaction Boundary-Layer Equations

M. J. Werle* and S. F. Wornom†
Virginia Polytechnic Institute and State University, Blacksburg, Va.

Introduction

Flügge-Lotz and Blottner[1] have numerically solved the hypersonic boundary-layer, displacement interaction problem; however, attention has recently been focused on the possible existence of a saddle point type behavior that can occur in this class of problem. Garvine[2] observed saddle point behavior for the strong interaction problem when employing a viscous shock layer approach, and cites the boundary-layer solutions of Baum[3] as supporting his finding. However, several recent studies[4–6] did not encounter this difficulty, thereby giving impetus to a reapplication of Flügge-Lotz and Blottner's[1] original concepts to the boundary-layer equations to test their generality. The present study finds that the basic implicit finite difference approach originally proposed in Ref. 1 provides a basis for obtaining solutions to virtually any strong interaction problem. Solutions are given for a wide range of flow conditions without the adverse saddle point type behavior predicted by Ref. 2.

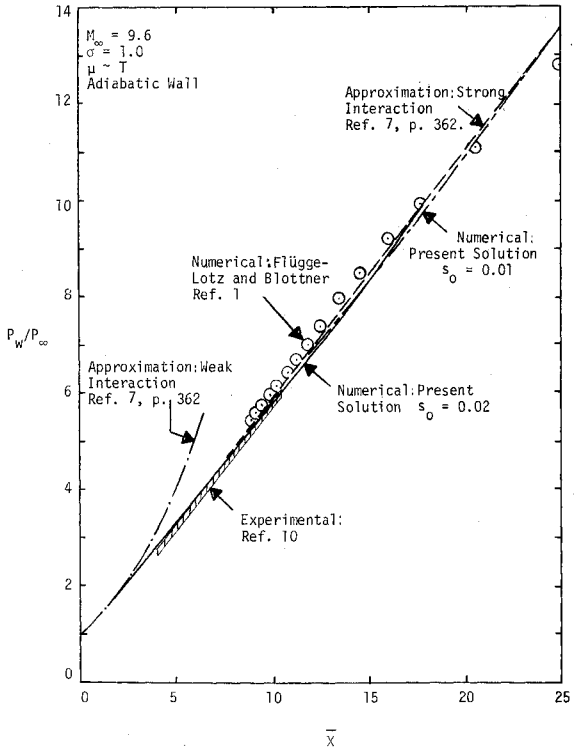

Fig. 1 Surface pressure distribution at $M_\infty = 9.6$.

Governing Equations

The simplest statement of the problem results from using Levy Lees type variables where the independent variables are defined in terms of the nondimensional physical variables as follows

$$\xi = \int_0^s \rho_e \mu_e U_e ds \quad \eta = \frac{U_e}{(2\xi)^{1/2}} \int_0^N \rho dN \tag{1}$$

where s and N are the usual boundary-layer coordinates along and normal to the surface, ρ,μ and U the density, viscosity, and velocity respectively with the subscript e referring to the inviscid flow's edge values.

In addition, the viscous region's velocity, u, total enthalpy, H, and viscosity function, $\rho\mu$, are normalized through the definitions

$$F = u/U_e \quad g = H/H_e \quad l = \rho\mu/\rho_e\mu_e \tag{2}$$

for which the governing equations become

Continuity

$$F + 2\xi F_\xi + V_\eta = 0 \tag{3a}$$

Momentum

$$(lF_\eta)_\eta - VF_\eta + (1 + \alpha/2)\beta(g - F^2) - 2\xi FF_\xi = 0 \tag{3b}$$

and Energy

$$(1/\sigma)(lg_\eta)_\eta - Vg_\eta + (lFF_\eta)_\eta(1 - 1/\sigma)\,2\alpha/(2 + \alpha) - 2\xi Fg_\xi = 0 \tag{3c}$$

where the Prandtl number, σ, is assumed constant. In these equations the inviscid flow influence is contained in ξ,α, and β, where

$$\alpha = U_e^2/[H_e - (1/2)U_e^2] \quad \beta = (2\xi/U_e)(dU_e/d\xi) \tag{4}$$

The tangent wedge rule[7] is used to predict the inviscid flow pressure. Using this, the isentropic relations, and Euler's equation we obtain a direct relation between α and the displacement thickness slope, with a similar statement for β in terms of the second derivative of the displacement thickness. Thus the system of equations is closed, and a solution can be obtained at any station along a surface so long as one is known at some upstream point.

Numerical Method

The method used for obtaining solutions to Eqs. (3a–3c) is the implicit finite difference scheme developed by Flügge-Lotz and Blottner[1] with modifications by Davis.[8] Given the solution at any streamwise location, as well as the inviscid edge values of ξ,α, and β at an incremental ξ step forward, this method straight-forwardly obtains the boundary-layer profiles at the new location using finite difference representations of all partial derivatives. The interaction process between the boundary-layer growth and the inviscid mainstream is accounted for by using an iterative scheme which

Received December 21, 1971; revision received May 10, 1971. This work was supported by ONR under Contract N00014-70-C-0024.

Index category: Boundary Layers and Convective Heat Transfer—Laminar.

* Assistant Professor, Department of Engineering Mechanics.
† Graduate Research Assistant, Department of Engineering Mechanics.

essentially guesses the edge flow state at the new station, computes the boundary-layer characteristics under these conditions, re-evaluates the edge values with the tangent wedge pressure law, and repeats the cycle until convergence is achieved to within some reasonable level. Initialization of the method is accomplished by following the lead of Ref. 1, wherein the strong interaction solution delineated by Stewartson[9] is imposed at the first station which itself is chosen such that the hypersonic interaction parameter $\bar{\chi}$ is on the order of 20–25. This solution is recovered from equations (3a–3c) by droping all ξ derivatives and noting that in the hypersonic limit, $\alpha \to \infty$ and $\beta \to 0$ such that $(1 + \alpha/2)\beta \to (\gamma - 1)/\gamma$, where γ is the specific heat ratio. This produces a set of ordinary differential equations easily integrated using the present difference scheme.

Results and Discussion

The first comparison is with Flügge-Lotz and Blottner[1] since this appears to be the only case to date solved numerically without branching type behavior. Figure 1 shows that the computed values of the wall pressure ratio P_w/P_∞, display no inclination toward a branching behavior while reasonably tracing the expected strong interaction behavior. A small initial departure from the linear dependence occurred, but damped quickly with only slight residual effects further downstream. The position chosen for the initialization of the solution, s_o, also seemed to have only a secondary effect on the solution further downstream as one notes that the effect of changing from $s_o = 0.01$ to $s_o = 0.02$ disappears by $\bar{\chi} = 15$ in both cases. Favorable comparisons are also given with Flügge-Lotz and Blottner's earlier results[1] as well as with the experimental data.[10] The difference between the present method and Flügge-Lotz and Blottner's results stems directly from the fact that they initialized their solution using the first order estimate of the strong interaction solution whereas the present effort employed second order terms as well.

One remaining point with regard to these solutions concerns the appearance of an oscillatory instability in the surface pressure with downstream progression. Cheng et al.[6] observed a similar occurrence when numerically marching away from a flat plate leading edge using the fully viscous shock layer equations. They found that as they entered the strong interaction region from the merged-layer region, numerical instabilities entered the solutions through the continuity equation. This behavior was attributed to diminishing wall slip influence and subsequent loss in accuracy of the integration technique used for the continuity equation. Similar instabilities were observed in the present work and, as in Ref. 6, these first appeared at the base of the V velocity profile obtained when integrating Eq. (3a). Such behavior was effectively filtered herein by an averaging technique such that the value of V at a point, η, was obtained by integrating Eq. (3a) outward from the wall using the trapezoid rule, and

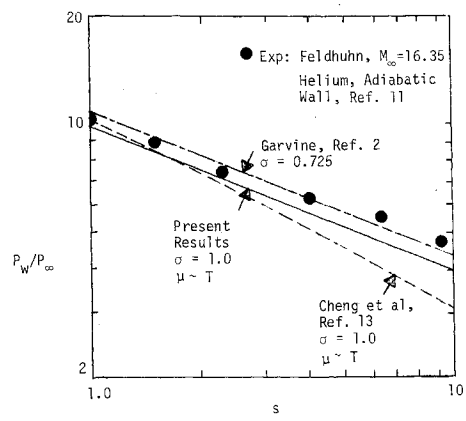

Fig. 2 Comparison with experiment at $M_\infty = 16$.

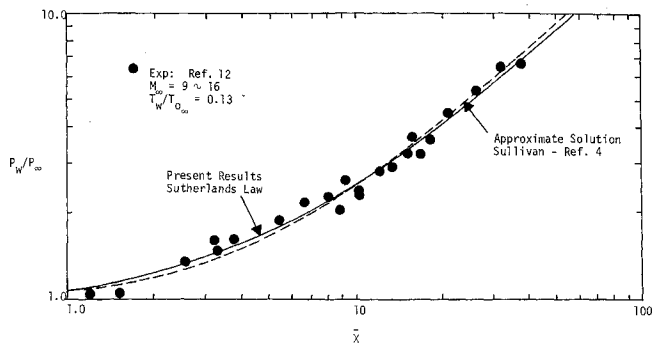

Fig. 3 Comparisons with cold wall experimental data.

averaging this value with that of V at the same η one ξ station back. In regions with no oscillations, the averaging caused negligible change in the solutions (as one might expect for small step sizes), but it effectively purged the solutions of all high-frequency oscillations.

The second case considered herein was also studied by Garvine[2] and corresponds to the experimental study of Feldhuhn.[11] Garvine,[2] in studying this problem using a set of fully viscous shock layer equations, encountered a strong branching behavior as integration proceeded downstream. Figure 2 compares the present results with the envelope of branching solutions obtained by Garvine. Note that no tendency toward branching appears, and that the comparison with experiment is acceptable enough to verify the present technique. It should be pointed out that without using the averaging in the continuity equation, a strong oscillation occurred in this solution. Apparently, the amplification process discussed earlier is also present in these solutions and must be damped to allow smooth transition with the downstream solution.

The final comparison, in Fig. 3, is with the approximate solutions of Sullivan,[4] and a representative set of experimental results for a wide range of Mach numbers. The present results virtually duplicate both Sullivan's and the experimental results over the entire range of $\bar{\chi}$.

Conclusion

The numerical solution of the hypersonic strong interaction boundary-layer problem is not complicated by the saddle point behavior predicted by Ref. 2, and the basic numerical scheme of Flügge-Lotz and Blottner[1] is capable of handling this problem. Although an oscillatory instability occurred, this was easily damped with an averaging technique in the continuity equation. Solutions were obtained for a wide enough range of Mach numbers and wall temperatures to reasonably prove the validity of the approach.

References

[1] Flügge-Lotz, I. and Blottner, F. G., "Computation of the Compressible Laminar Boundary-Layer Flow Including Displacement Thickness Interaction Using Finite Difference Methods," TR 131, Jan. 1962, Stanford Univ., Stanford, Calif.

[2] Garvine, R. W., "Upstream Influence in Viscous Interaction Problems," *The Physics of Fluids*, Vol. 11, No. 7, July 1968, pp. 1413–1423.

[3] Baum, Eric, "An Interaction Model of a Supersonic Laminar Boundary Layer on Sharp and Rounded Backward Facing Steps," *AIAA Journal*, Vol. 6, No. 3, March 1968, pp. 440–447.

[4] Sullivan, P. A., "Interaction of a Laminar Hypersonic Boundary Layer and a Corner Expansion Wave," *AIAA Journal*, Vol. 8, No. 4, April 1970, pp. 765–771.

[5] Stollery, John L., "Hypersonic Viscous Interaction on Curved Surfaces," AIAA Paper 70-782, Los Angeles, Calif., June 1970.

[6] Cheng, H. K., Chen, S. Y., Mobley, R., and Huber, C. R., "The Viscous Hypersonic Slender-Body Problem: A Numerical Approach Based on a System of Composite Equations," Memo. RM-6193-PR, May 1970, The Rand Corp., Santa Monica, Calif.

[7] Hayes, W. D. and Probstein, R. F., *Hypersonic Flow Theory*, Academic Press, New York, 1959.

[8] Davis, R. T., "Numerical Solution of the Hypersonic Viscous Shock-Layer Equations," *AIAA Journal*, Vol. 8, No. 5, May 1970, pp. 843–851.

[9] Stewartson, K., "On the Motion of a Flat Plate at High Speed in a Viscous Compressible Fluid—II Steady Motion," *Journal of the Aeronautical Sciences*, Vol. 22, No. 5, 1955, pp. 303–309.

[10] Bertram, M. H. and Blackstock, T. A., "Some Simple Solutions to the Problem of Predicting Boundary-Layer Self Induced Pressures," TN D-798, April 1961, NASA.

[11] Feldhuhn, R. H., "An Experimental Investigation of the Effects of Leading Edge Reynolds Number and Angle of Attack of the Flow of Helium Over a Flat Plate at M = 16.35," Internal Memo. 8, July 1965, Dept. of Aerospace and Mechanical Sciences, Gas Dynamics Lab., Princeton Univ., Princeton, N. J.

[12] Hall, J. G. and Golian, T. C., "Shock Tunnel Studies of Hypersonic Flat Plate Air Flow," Rept. AD-1052-A-10, 1960, Cornell Aerospace Lab., Buffalo, N. Y.

[13] Cheng, H. K., Hall, J. G., Golian, T. C., and Hertzberg, A., "Boundary Layer Displacement and Leading-Edge Bluntness Effects in High Temperature Hypersonic Flow," *Journal of the Aerospace Sciences*, Vol. 28, No. 5, 1961, pp. 353–381.

Molecular Beam Extraction from Equilibrium Gas Flows

ULF BOSSEL*
DFVLR-AVA, Göttingen, West Germany

Theory

CONSIDER the beam system schematic, Fig. 1. If density-sensitive detectors are used, as in the present case, then the beam properties are found as the moments of the distribution describing the state of the gas inside the beam source region from which the beam molecules are isolated. For flux-sensitive devices the detection signal should be proportional to the moments of the distribution function augmented factorially by a detection, or plane crossing probability $(\mathbf{c}\cdot\mathbf{v})$, the scalar product of the molecular velocity $\mathbf{c}$ and the plane normal $\mathbf{v}$. Here the concept of an escape probability associated with beam formation in conventional studies has been generalized to a plane-crossing probability associated with particular detection techniques. The results of the obvious integrations over small solid angles $0 < \Omega \equiv A_s/L^2 \ll 4\pi$ are listed in Table 1, since no comprehensive tabulation can be found elsewhere.

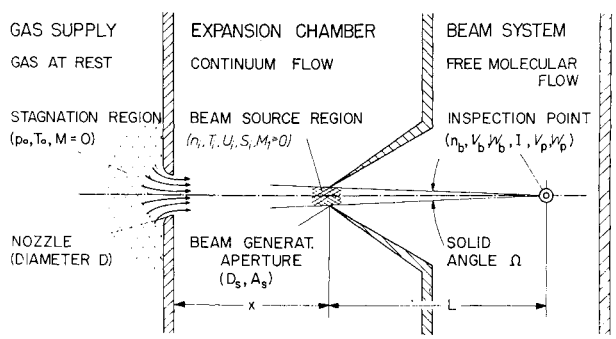

Fig. 1 Schematic of beam generation system.

Received June 18, 1970; revision received June 8, 1971. Experiments carried out at the University of California, Berkeley, Calif., and numerical work conducted at Syracuse University were combined at Göttingen. The author gratefully acknowledges support of all three institutions.

Index categories: Rarefied Flows; Supersonic and Hypersonic Flow; Atomic, Molecular, and Plasma Properties.

* Research Scientist, Department of Space Aerodynamics.

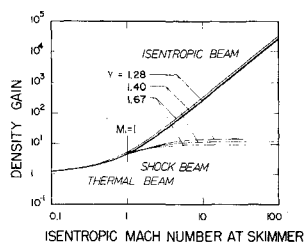

Fig. 2 Density gain vs isentropic skimmer Mach number.

Skimming Models

Two extreme cases are considered for the isolation of nozzle beams from equilibrium gas flows. The isentropic model[1] neglects interference of the skimmer with the incoming flow. The beam source conditions, index 1, are related to the stagnation region via the isentropic expansion laws. If the flow is completely randomized prior to beam formation by either a normal shock ahead of, or at the skimmer, or by diffuse adiabatic scattering inside the skimmer, then the isentropic laws are augmented by the Rankine-Hugoniot relations. The shock-beam[2] properties therefore deserve the index 2. Consequently, the density n_i, temperature T_i and molecular speed ratio S_i in Table 1 must be replaced by the appropriate beam source conditions depending on the case considered.

Figures 2 and 3 illustrate the nature of shock beams. They are neither supersonic, nor effusive, but could be classified as subsonic nonisentropic beams. Figure 2 shows that such beams are denser than effusive reference beams from a thermal source at isentropic freestream density n_1. Naturally, they are less dense than isentropic supersonic beams because of the partial loss of precollimation during the shock transition. The significance of the branchpoit at $M_1 = 1$ is obvious. The shock beam formation requires $M_1 \geqq 1$.

Similarly, Fig. 3 reveals that the average velocity V_b of diatomic shock beam molecules is between that of an effusive and an isentropic supersonic beam. Whereas $V_{b,1}$ and the isentropic drift U_1 merge at higher skimmer Mach numbers M_1 $V_{b,2}$ remains significantly greater than U_2 indicating that effusive phenomena dominate in the shock beam formation.

Experimental Results

The experimental setup has been described elsewhere.[3] Only the near-inviscid portion ($8000 < Re^* \equiv \rho^* Da^*/\mu^* < 50{,}000$) of the slender 0.027 cm skimmer data are checked against theory. The observed beam density data are presented in Fig. 4 as a function of the computed total number flux $\dot{N}_{tot}$ into the skimmer and the stagnation pressure p_0. We wish to demonstrate that the outer maxima near D relate

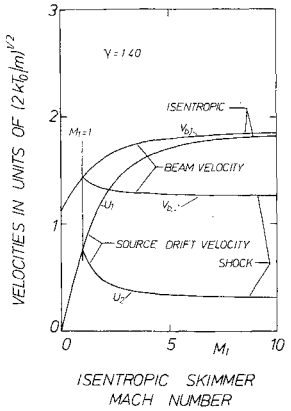

Fig. 3 Comparison of beam and source drift velocities.